Neutrino masses, flavor anomalies, and muon $g-2$ from dark loops

Ricardo Cepedello,[1,*] Pablo Escribano,[2,3,†] and Avelino Vicente[2,3,‡]

[1]*Institut für Theoretische Physik und Astrophysik, Universität Würzburg, 97074 Würzburg, Germany*
[2]*Instituto de Física Corpuscular, CSIC-Universitat de València, 46980 Paterna, Spain*
[3]*Departament de Física Teòrica, Universitat de València, 46100 Burjassot, Spain*

(Received 24 September 2022; accepted 6 February 2023; published 27 February 2023)

The lepton sector of the Standard Model is at present haunted by several intriguing anomalies, including an emerging pattern of deviations in $b \to s\ell\ell$ processes, with hints of lepton flavor universality violation, and a discrepancy in the muon anomalous magnetic moment. More importantly, it cannot explain neutrino oscillation data, which necessarily imply the existence of nonzero neutrino masses and lepton mixings. We propose a model that accommodates all the aforementioned anomalies, induces neutrino masses and provides a testable dark matter candidate. This is achieved by introducing a dark sector contributing to the observables of interest at the 1-loop level. Our setup provides a very economical explanation to all these open questions in particle physics and is compatible with the current experimental constraints.

DOI: 10.1103/PhysRevD.107.035034

I. INTRODUCTION

Several anomalies are currently hinting at the presence of new physics in the lepton sector of the Standard Model (SM). First of all, neutrino oscillation experiments have clearly established that neutrinos are massive. This is arguably the most robust evidence of new physics (NP) beyond the SM. It definitely calls for an extension of the SM lepton sector with new degrees of freedom which, in most scenarios, lead to deviations in other observables, directly associated to leptons or not. Interestingly, other anomalies have recently showed up, mainly involving the muon:

(i) The hints observed in $b \to s$ transitions, which already point toward an emerging pattern [1–3]. This includes a deviation in the branching ratio $\mathrm{Br}(B_s \to \mu\bar{\mu})$ [4–7] (although the very recent CMS result [8] is in good agreement with the SM) and, especially, the possible violation of lepton flavor universality in B-meson decays [9–12] encoded in the $R_{K^{(*)}}$ ratios, defined as

$$R_{K^{(*)}} = \frac{\mathrm{Br}(B \to K^{(*)}\mu\bar{\mu})}{\mathrm{Br}(B \to K^{(*)}e\bar{e})}. \tag{1}$$

For these ratios, the theoretical uncertainties of the SM predictions are at the percent level [13], which strengthens the relevance of the anomalies.

(ii) The muon anomalous magnetic moment $a_\mu = (g-2)_\mu/2$ has been recently measured with unprecedented accuracy [14] and in agreement with previous measurements from the E821 experiment [15]. The combination of both observed values yields a deviation of 4.2σ from the SM predictions [16],[1]

$$\Delta a_\mu = a_\mu^{\mathrm{exp}} - a_\mu^{\mathrm{SM}} = (2.51 \pm 0.59) \times 10^{-9}. \tag{2}$$

Finally, the nature of the dark matter (DM) that constitutes ~25% of the energy content of the Universe is still a mystery. Many new physics models include DM candidates, sometimes relating them to other open questions in particle physics or even being instrumental in their resolution. While these NP indications might have different origins, and some of them are still hints to be confirmed with further experimental data and improved theoretical calculations, it is tempting to consider a common explanation.

In this paper we introduce an economical, yet powerful model that provides an explanation to all these new physics indications. This is achieved thanks to the addition of a dark sector composed by a fermion singlet N, two generations of inert doublets η, a doublet leptoquark S and a singlet scalar ϕ, with the quantum numbers under $(\mathrm{SU}(3)_c, \mathrm{SU}(2)_L)_{\mathrm{U}(1)_Y}$

*ricardo.cepedello@physik.uni-wuerzburg.de
†pablo.escribano@ific.uv.es
‡avelino.vicente@ific.uv.es

[1]One should note, however, that the SM prediction is currently under debate due to recent lattice results [17–19].

$$N \sim (\mathbf{1},\mathbf{1})_0, \qquad \eta \sim (\mathbf{1},\mathbf{2})_{\frac{1}{2}}, \qquad S \sim (\mathbf{3},\mathbf{2})_{\frac{1}{6}},$$
$$\phi \sim (\mathbf{1},\mathbf{1})_{-1}. \tag{3}$$

The model also includes a dark $\mathbb{Z}_2$ parity, under which all the new fields are assumed to be odd, while the SM fields are even. This characterizes the dark sector of the model.[2] These ingredients are enough to induce neutrino masses, accommodate the $b \to s\ell\ell$ and $(g-2)_\mu$ anomalies, and provide a viable DM candidate, while being compatible with all the relevant experimental constraints. To the best of our knowledge, our economical model is the first to take into account all these unresolved issues in the lepton sector *simultaneously* and, as a by-product, also address the long-standing DM problem. In our scenario, all NP contributions to the observables of interest are induced at the 1-loop level, with $\mathbb{Z}_2$-odd particles running in the loop. These *dark loops* characterize our setup.

The connection between neutrino masses and the anomalies in $b \to s$ transitions has been explored in several works. In most cases, neutrino masses are generated radiatively with leptoquarks participating in the loop. These leptoquarks are then responsible for explaining at tree-level the flavor anomalies [20–22], and the $(g-2)_\mu$ [23–30]. Reference [31] proposes an explanation for the $b \to s\ell\ell$ anomalies via loops, also linked to the generation of neutrino masses, while Ref. [32] considers a left-right model with neutrino masses generated through an inverse seesaw. Finally, the $b \to s$ anomalies have also been discussed in connection to the dark matter problem. We would like to highlight Refs. [33–36], which also address the $b \to s\ell\ell$ and $(g-2)_\mu$ anomalies via loops involving DM, and refer to the review [37] for other works in this direction.

II. THE MODEL

The new states in our model allow us to write the additional Lagrangian terms:

$$-\mathcal{L}_{\rm NP} = Y_N \bar{N} \ell_L \eta + Y_S \bar{q}_L S N + \kappa \overline{N^c} e_R \phi^\dagger + \frac{1}{2} M_N \overline{N^c} N + \text{H.c.} \tag{4}$$

Here Y_N is a 3×2 matrix, Y_S and κ are both 3-components vectors, while M_N is a parameter with dimensions of mass. Additional Yukawa couplings not written here are forbidden by the dark $\mathbb{Z}_2$ parity. For instance, this is the case of the $\overline{N}\ell_L H$ or $\bar{d}_R \ell_L S$ terms. The scalar potential of the model also contains new terms, including two that will be relevant for the discussion:

$$\mathcal{V}_{\rm NP} \supset \frac{\lambda_5}{2}(H^\dagger \eta)^2 + \mu H \eta \phi + \text{H.c.} \tag{5}$$

[2]We use the term *dark* to refer to any particle charged under the $\mathbb{Z}_2$ symmetry.

We remind the reader that two η doublets are added to the field inventory of the model. Therefore, μ is a 2-component vector, while λ_5 is a 2×2 symmetric matrix. In the following, only the SM scalar doublet H will be assumed to acquire a nonzero vacuum expectation value (VEV), $H^0 = v/\sqrt{2}$, where $v \simeq 246$ GeV is the electroweak VEV. This preserves the $\mathbb{Z}_2$ dark parity.

Neutrino masses The conservation of $\mathbb{Z}_2$ prevents the generation of neutrino masses at tree-level. However, the simultaneous presence of Y_N, M_N and λ_5 in Eqs. (4) and (5) implies the explicit breaking of lepton number in two units. Majorana neutrino masses are induced at the 1-loop level *á la Scotogenic* [38], as shown in Fig. 1. The states running in the loop belong to the dark sector, a feature enforced by the $\mathbb{Z}_2$ symmetry and common to all NP contributions discussed below. The resulting neutrino masses in the limit of small λ_5 is given by [39]

$$(m_\nu)_{\alpha\beta} \approx \frac{1}{32\pi^2} v^2 \sum_{a,b} (Y_N)_{\alpha a}(Y_N)_{\beta b} \lambda_5^{ab} \frac{M_N}{m_b^2 - M_N^2} \times \left[\frac{m_b^2}{m_a^2 - m_b^2}\log\frac{m_a^2}{m_b^2} - \frac{M_N^2}{m_a^2 - M_N^2}\log\frac{m_a^2}{M_N^2}\right], \tag{6}$$

were $m_{a,b}$ are the masses of the two η doublets. This can be roughly estimated as $m_\nu \sim \frac{\lambda_5 Y_N^2 v^2}{16\pi^2 M_N}$. Therefore, we obtain two nonzero neutrino masses with $m_\nu \sim 0.1$ eV for $M_N = 1$ TeV and $\lambda_5^{ab} \sim 10^{-10}$, if the entries of the Y_N matrix are of order 1. The smallness of the λ_5 elements is technically natural and protected against radiative corrections [40], since in the limit $\lambda_5^{ab} \to 0$ lepton number is restored.

III. OBSERVABLES

We now discuss the NP contributions induced by the new states in our model to the observables of interest.

$b \to s\ell\ell$ anomalies The model induces many 1-loop contributions to $b \to s\ell\ell$ observables. Some examples of them are shown in Fig. 1. We note that the charged η^- scalars mix with the charged singlet ϕ^-, and thus the states propagating in the loops are the mass eigenstates resulting from this mixing. We nevertheless show gauge eigenstates in Fig. 1 to better illustrate the most relevant contributions. Box diagrams are responsible for flavor universality violating contributions, central to explain observables such as the R_K ratio. In addition, one should also consider flavor universal contributions from penguin diagrams, as shown in the second row of Fig. 1. Our model realizes scenario (b) of [41]. We highlight the presence of the crossed-diagram in Fig. 1, possible due to the Majorana nature of the N singlets. We do not show an analogous crossed-diagram with ϕ^- in the loop. These diagrams play a crucial role in canceling unwanted contributions to $B_s - \bar{B}_s$ mixing [42], as discussed below.

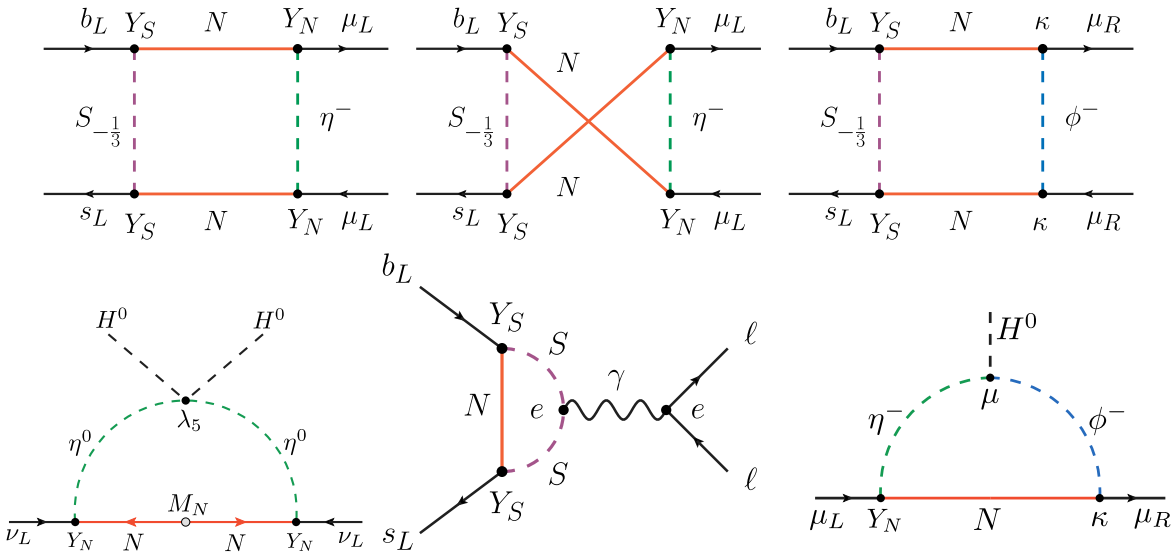

FIG. 1. Some NP contributions to the observables of interest. Above: Box diagrams contributing to $b \to s\mu\mu$ observables. Below from left: Generation of neutrino masses at the 1-loop level, η^0 represents the real and imaginary components of all generations of η^0; flavor-universal penguin contribution to the $b \to s\ell\ell$ anomalies; and 1-loop contribution to the anomalous magnetic moment of the muon (photon line should be attached to the charged scalars). Other contributions, not shown here for simplicity, were considered in the analysis.

Anomalous magnetic moment of the muon The model also has new contributions to the anomalous magnetic moment of the muon, as shown in the lower row of Fig. 1. One should note that two different Yukawa couplings enter this diagram. While Y_N plays a role in the generation of neutrino masses, the κ Yukawa couplings do not. We also highlight the presence of the μ trilinear couplings that induce mixing between the charged component of η and ϕ and can be used to chirally enhance the associated contribution. These NP contributions were computed using the formalism described in [43].

Dark matter Last but not least, the model also provides a solution to the DM problem. The lightest $\mathbb{Z}_2$-odd state is stable and, if electrically neutral, it is a potentially valid DM candidate. Two possibilities arise: the lightest N state and one of the components (CP-even or CP-odd) of the neutral η^0 scalars. Both scenarios have been widely studied in the literature for the pure scotogenic model [38] and both have been shown to be compatible with the observed DM relic density. However, we note that the scalar candidate can achieve this more easily [44–48], since the fermionic candidate requires large Y_N Yukawa couplings and then leads to some tension with existing bounds from lepton flavor violating (LFV) observables [49]. We note, however, that our model deviates from the usual scenario with one inert η doublet, since two generations are introduced. This scenario was studied in great detail in [50], where it was shown that the richer inert sector may open up novel regions in parameter space where the relic density can match the observed value. For instance, this is achieved when both scalar doublets have similar masses since coannihilation rates get enhanced.

IV. NUMERICAL RESULTS

Our model faces several experimental constraints. First, we must make sure that neutrino oscillation data are correctly reproduced. We use the results of the global fit [51] and implement them by means of a Casas-Ibarra parametrization [52], properly adapted to the Scotogenic scenario [53–55]. This allows us to write the Y_N Yukawa matrix as

$$Y_N^T = V D_{\sqrt{\Sigma}} R D_{\sqrt{m_\nu}} U_{\mathrm{PMNS}}^\dagger, \tag{7}$$

where R is a general 2×3 orthogonal matrix defined as

$$R = \begin{pmatrix} 0 & \cos\theta & -\sin\theta \\ 0 & \sin\theta & \cos\theta \end{pmatrix}. \tag{8}$$

D_X represents the diagonal form of the matrix X, while Σ is defined from Eq. (6) as $m_\nu = Y_N \cdot \Sigma \cdot Y_N$, with V its diagonalization matrix. Finally, U_{PMNS} is the usual unitary matrix that relates neutrino flavor to mass eigenstates. Equation (7) illustrates an important connection in our model: neutrino masses strongly restrict the elements of the Y_N Yukawa matrix, which play a crucial role in the resolution of the $b \to s\ell\ell$ and $(g-2)_\mu$ anomalies (see Fig. 1). Furthermore, as in most neutrino mass models, LFV processes, such as $\mu \to e\gamma$, are potentially dangerous. Searches by the MEG collaboration have shown that the branching ratio for this radiative decay cannot exceed 4.2×10^{-13} [56].

Regarding processes with mesons, the main constraints come from $b \to s\gamma$, $B \to K^{(*)}\nu\bar{\nu}$ and $B_s - \bar{B}_s$ mixing. The $b \to s\gamma$ decays yield strong constraints on the coefficients of dipole operators [57]. These are induced at the 1-loop level by diagrams like the one shown in the lower left corner of Fig. 1, with photons or gluons and without the charged leptons. The inclusive $b \to s\gamma$ branching ratio is experimentally determined to be $\mathrm{BR}(b \to s\gamma) = (3.49 \pm 0.19) \times 10^{-4}$ [58]. As we will show below, this constrains the $(Y_S)_2 \times (Y_S)_3$ product. About $B \to K^{(*)}\nu\bar{\nu}$, note that if a contribution to $B \to K^{(*)}\ell^+\ell^-$ exists, the corresponding process with neutrinos is unavoidable due to $\mathrm{SU}(2)_\mathrm{L}$ invariance. Current experimental results set limits to the branching ratios of $B \to K^{(*)}\nu\bar{\nu}$ which, normalized to their SM predictions, are restricted to $R_K^{\nu\bar{\nu}} < 3.9$ and $R_{K^*}^{\nu\bar{\nu}} < 2.7$ [59]. On top of this, $B_s - \bar{B}_s$ mixing [60] is again inevitable and typically very constraining in scenarios aiming at an explanation of the $b \to s\ell\ell$ anomalies at the 1-loop level. Any model that generates a box diagram with b and s quarks and two leptons, like the ones in Fig. 1, will automatically produce box contributions to the four quarks operators responsible for $B_s - \bar{B}_s$ mixing. In fact, this specific constraint precludes most radiative models for $b \to s$ transitions. In our scenario, however, the Majorana nature of the N singlet can be used to suppress $B_s - \bar{B}_s$ mixing in the limit of (nearly) degenerate NP masses participating in the box, i.e. $S_{-1/3}$ and N, as pointed out in [42]. This is actually the reason to introduce just one N singlet. If the model contained more than one generation of N, the cancellation would not work anymore or would require more tunings.

We present now our results. Our goal is to prove that our model can accommodate all the anomalies while being consistent with neutrino oscillation data and all the experimental constraints. In what concerns the $b \to s\ell\ell$ anomalies, a reasonable goal is to accommodate scenario 5 of the global fit [3], characterized by

$$\begin{aligned} \mathcal{C}_{9\mu}^V &= -0.55^{+0.44}_{-0.47}, \\ \mathcal{C}_{10\mu}^V &= 0.49^{+0.35}_{-0.41}, \\ \mathcal{C}_9^U &= \mathcal{C}_{10}^U = -0.35^{+0.42}_{-0.38}, \end{aligned} \tag{9}$$

where $\mathcal{C}_9$ and $\mathcal{C}_{10}$ are the Wilson coefficients of the $\mathcal{O}_9 = (\bar{s}\gamma_\mu P_L b)(\bar{\ell}\gamma^\mu \ell)$ and $\mathcal{O}_{10} = (\bar{s}\gamma_\mu P_L b)(\bar{\ell}\gamma^\mu\gamma_5 \ell)$ effective operators, respectively. The superindices V and U denote flavor universality violating and conserving contributions, respectively, and the flavor universality violating ones are specific to the muon flavor. This scenario provides a clear improvement with respect to the SM in what concerns the description of $b \to s\ell\ell$ data [3]. We constructed a χ^2-function in the usual way, with these four Wilson coefficients and the anomalous magnetic moment of the muon. Rather than finding the global minimum of the resulting χ^2-function, which depends nontrivially on many model parameters, our goal is to prove that our model can provide a good explanation to all the anomalies. Therefore, in order to simplify the analysis, we fixed several parameters. First, the masses of the NP states were taken to be close to 1 TeV, a typical reference NP scale. We have explicitly checked that the qualitative results and the conclusions of our analysis remain the same with other choices of NP scale. Note that the $B_s - \bar{B}_s$ mixing suppression requires the masses of S and N to be degenerate or nearly degenerate [42]. The mass of η is taken to be lower, around 550 GeV. With this hierarchy, η would be the lightest stable particle with a mass compatible with the observed DM relic density and direct detection cross-section bounds [47,48]. We assumed that the 2×2 matrix λ_5 is proportional to the identity, i.e. $\lambda_5 = \lambda_5^0 \mathbb{I}_2$, and fix the following values:

$$\mu_1 = -\mu_2 = -1.0\ \mathrm{TeV}, \qquad \kappa_1 = 0, \tag{10}$$

$$\lambda_5^0 = 2 \times 10^{-10}, \qquad \kappa_2 = 0.04. \tag{11}$$

We noticed that these two elements of the coupling vector $\kappa = (\kappa_1\kappa_2\kappa_3)$ need to be small in order to suppress the branching ratio of $\mu \to e\gamma$ below the experimental bound. Indeed, we chose to set κ_1 to zero. The rest of the parameters of the model are not relevant for our discussion here, given the generation structure of the diagrams depicted in Fig. 1. Note also that due to the external quark structure, Y_S always enters in the combination $(Y_S)_2 \times (Y_S)_3$. For the χ^2 minimization, we are then left with $(Y_S)_2 \times (Y_S)_3$ and $\sin\theta$. We found that the values of the parameters for which χ^2 was minimal, were

$$(Y_S)_2 \times (Y_S)_3 = 0.6, \qquad \sin\theta = 0.25, \tag{12}$$

giving $\chi^2_{\mathrm{min}} = 1.52$ and $\Delta\chi^2 = \chi^2_{\mathrm{SM}} - \chi^2_{\mathrm{min}} = 21.23$. This not only shows a remarkable improvement with respect to the SM, but the low χ^2_{min} value also guarantees that all the anomalous observables can be properly accommodated in our model. This is better illustrated on the left-hand side of Fig. 2, which shows the results of our χ^2 fit in the $\sin\theta - (Y_S)_2 \times (Y_S)_3$ plane. We find that both parameters can substantially deviate from their best-fit values without affecting the χ^2-function notably. However, $\sin\theta$ is required to be in the 0.25 ballpark in order to reduce the $\mu \to e\gamma$ branching ratio below its experimental bound. This turns out to be a strong constraint in our model due to the connection to neutrino masses, which generically require the Y_N couplings involving the electron to be nonzero. Similarly, the $b \to s\gamma$ constraint imposes an upper bound on the $(Y_S)_2 \times (Y_S)_3$ product, which has to be below $\sim$1. The impact on $\mathcal{C}_{9\mu}^V$ and Δa_μ is shown on the right-hand side of Fig. 2. Here we see that the central value for both *observables* (we treat the $\mathcal{C}_{9\mu}^V$ coefficient as an observable here) can be easily achieved in our model and is in fact very close to our global best-fit point in Eq. (9), which only deviates slightly due to the influence of

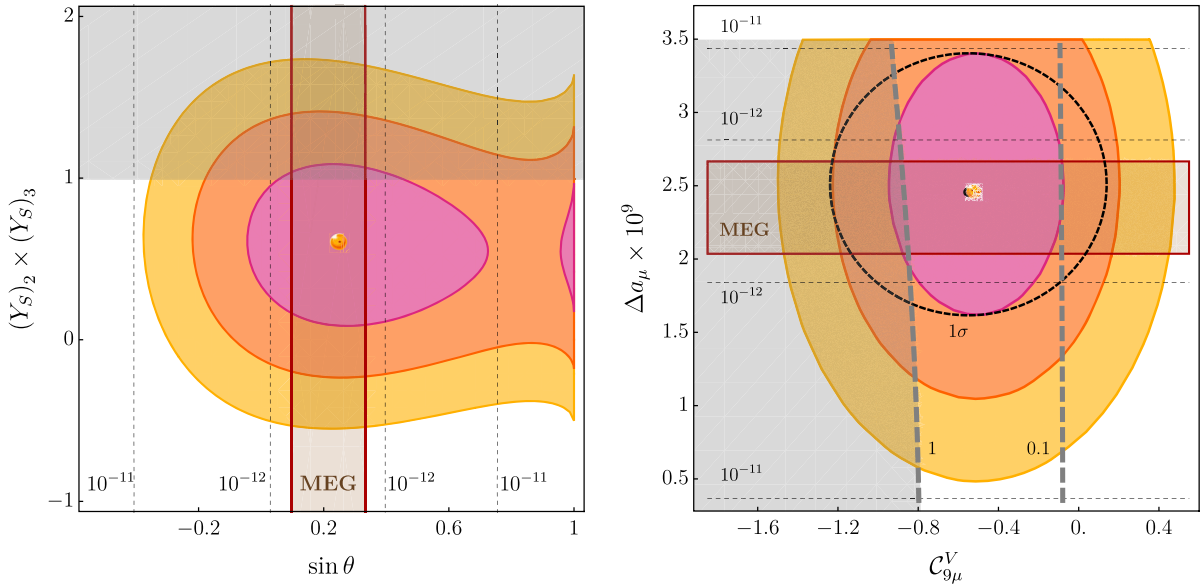

FIG. 2. Results of our χ^2 fit of the model parameters. The colored regions correspond to 1σ (pink), 2σ (orange) and 3σ (yellow) regions, while the best-fit point is indicated with an orange dot. The region allowed by the MEG experiment is shown in dark red, while the dashed lines correspond to contours of $\mathrm{Br}(\mu \to e\gamma)$. The shaded region is excluded by the $b \to s\gamma$ constraint at 3σ. In the right panel, contours of the $(Y_S)_2 \times (Y_S)_3$ product are shown with thick dashed gray lines, while the black dashed line and dot are the experimentally determined 1σ region and central value, respectively.

other Wilson coefficients. It is also remarkable that our model does not require too large Y_S Yukawa parameters to accommodate the $b \to s\ell\ell$ anomalies. In fact, $\mathcal{O}(1)Y_S$ Yukawas are sufficient to reproduce all the anomalies at the 1σ level. We emphasize once again that all the parameter points considered in our analysis comply with the constraints from neutrino oscillation data, $b \to s\gamma$ and $B_s - \bar{B}_s$ mixing. The $B \to K^{(*)}\nu\bar{\nu}$ bounds are also easily satisfied. Finally, the mass spectrum chosen in our numerical fit also accommodates the observed DM relic density. Therefore, although a more sophisticated analysis is required to determine precisely the region of parameter space where our model can accommodate all the anomalies, we have shown that this region does exist and the model can fully achieve its goals.

V. DISCUSSION

We have proposed a novel model that accommodates the existing deviations in $b \to s\ell\ell$ observables and the muon $g-2$, induces neutrino masses and provides a weakly interacting dark matter candidate, thanks to a dark sector including several states contributing to the observables of interest at the 1-loop level. We have shown that our simple and economical model can explain all the anomalies via these dark loops. This is achieved with renormalizable Yukawa couplings, while being compatible with neutrino oscillation data and the existing experimental bounds. The flavor violating muon decay $\mu \to e\gamma$ turns out to provide an important constraint, but this can be easily satisfied in a wide region of the parameter space.

The scenario considered in our analysis requires the existence of several states at the TeV scale. Since they are all odd under a new dark parity, their production and decay channels are modified with respect to more common scenarios. For instance, the S leptoquark must be produced in pairs at colliders and subsequently decay as $S \to jN \to j\ell\not{E}_T$, where the jet can be given by a 2nd or 3rd generation quark and the missing energy in the final state is due to the production of the η DM particle. The approximate mass degeneracy between S and N, introduced to suppress $B_s - \bar{B}_s$ mixing, implies very soft jets, undetectable at the LHC. Moreover, if both η generations are lighter than N, additional leptons can be produced in the cascade. A more compressed spectrum would not affect our results in a substantial way, but would make these leptons very soft too, leading to a particularly challenging scenario at the LHC. In what concerns the heavy neutral lepton N, the conservation of the dark parity forbids its mixing with the standard neutrinos. We conclude that our scenario contains several nonstandard features and a dedicated study is thus required to fully assess its observability. We leave it for future work.

ACKNOWLEDGMENTS

Work supported by the Spanish Grants No. PID2020–113775GB-I00 (AEI) and No. CIPROM/2021/054 (Generalitat Valenciana). A. V. acknowledges financial support from MINECO through the Ramón y Cajal contract No. RYC2018-025795-I. R. C. is supported by the Alexander von Humboldt Foundation Fellowship. The work of P. E. is supported by the Formación de Personal Investigador (FPI) Grant No. PRE2018-084599.

[1] W. Altmannshofer and P. Stangl, Eur. Phys. J. C **81**, 952 (2021).
[2] T. Hurth, F. Mahmoudi, D. M. Santos, and S. Neshatpour, Phys. Lett. B **824**, 136838 (2022).
[3] M. Algueró, B. Capdevila, S. Descotes-Genon, J. Matias, and M. Novoa-Brunet, Eur. Phys. J. C **82**, 326 (2022).
[4] R. Aaij *et al.* (LHCb Collaboration), J. High Energy Phys. 09 (2015) 179.
[5] R. Aaij *et al.* (LHCb Collaboration), Phys. Rev. Lett. **118**, 191801 (2017).
[6] M. Aaboud *et al.* (ATLAS Collaboration), J. High Energy Phys. 04 (2019) 098.
[7] R. Aaij *et al.* (LHCb Collaboration), Phys. Rev. Lett. **128**, 041801 (2022).
[8] CMS Collaboration, Report No. CMS-PAS-BPH-21-006, 2022.
[9] R. Aaij *et al.* (LHCb Collaboration), J. High Energy Phys. 08 (2017) 055.
[10] S. Choudhury *et al.* (BELLE Collaboration), J. High Energy Phys. 03 (2021) 105.
[11] A. Abdesselam *et al.* (Belle Collaboration), Phys. Rev. Lett. **126**, 161801 (2021).
[12] R. Aaij *et al.* (LHCb Collaboration), Nat. Phys. **18**, 277 (2022).
[13] M. Bordone, G. Isidori, and A. Pattori, Eur. Phys. J. C **76**, 440 (2016).
[14] B. Abi *et al.* (Muon g-2 Collaboration), Phys. Rev. Lett. **126**, 141801 (2021).
[15] G. W. Bennett *et al.* (Muon g-2 Collaboration), Phys. Rev. D **73**, 072003 (2006).
[16] T. Aoyama *et al.*, Phys. Rep. **887**, 1 (2020).
[17] S. Borsanyi *et al.*, Nature (London) **593**, 51 (2021).
[18] M. Cè *et al.*, Phys. Rev. D **106**, 114502 (2022).
[19] C. Alexandrou *et al.*, arXiv:2206.15084.
[20] H. Päs and E. Schumacher, Phys. Rev. D **92**, 114025 (2015).
[21] S. Saad and A. Thapa, Phys. Rev. D **102**, 015014 (2020).
[22] S.-P. Li, X.-Q. Li, X.-S. Yan, and Y.-D. Yang, Eur. Phys. J. C **82**, 1078 (2022).
[23] O. Popov and G. A. White, Nucl. Phys. **B923**, 324 (2017).
[24] I. Bigaran, J. Gargalionis, and R. R. Volkas, J. High Energy Phys. 10 (2019) 106.
[25] S. Saad, Phys. Rev. D **102**, 015019 (2020).
[26] W.-F. Chang, J. High Energy Phys. 09 (2021) 043.
[27] T. Nomura and H. Okada, Phys. Rev. D **104**, 035042 (2021).
[28] J. Julio, S. Saad, and A. Thapa, Phys. Rev. D **106**, 055003 (2022).
[29] T. A. Chowdhury and S. Saad, Phys. Rev. D **106**, 055017 (2022).
[30] S.-L. Chen, W.-w. Jiang, and Z.-K. Liu, Eur. Phys. J. C **82**, 959 (2022).
[31] F. F. Freitas, J. a. Gonçalves, A. P. Morais, R. Pasechnik, and W. Porod, arXiv:2206.01674.
[32] M. Ashry, K. Ezzat, and S. Khalil, arXiv:2207.05828.
[33] D. Huang, A. P. Morais, and R. Santos, Phys. Rev. D **102**, 075009 (2020).
[34] G. Arcadi, L. Calibbi, M. Fedele, and F. Mescia, Phys. Rev. Lett. **127**, 061802 (2021).
[35] M. Becker, D. Döring, S. Karmakar, and H. Päs, Eur. Phys. J. C **81**, 1053 (2021).
[36] R. Capucha, D. Huang, T. Lopes, and R. Santos, Phys. Rev. D **106**, 095032 (2022).
[37] A. Vicente, Adv. High Energy Phys. **2018**, 3905848 (2018).
[38] E. Ma, Phys. Rev. D **73**, 077301 (2006).
[39] P. Escribano, M. Reig, and A. Vicente, J. High Energy Phys. 07 (2020) 097.
[40] G. 't Hooft, NATO Sci. Ser. B **59**, 135 (1980).
[41] P. Arnan, L. Hofer, F. Mescia, and A. Crivellin, J. High Energy Phys. 04 (2017) 043.
[42] P. Arnan, A. Crivellin, M. Fedele, and F. Mescia, J. High Energy Phys. 06 (2019) 118.
[43] A. Crivellin, M. Hoferichter, and P. Schmidt-Wellenburg, Phys. Rev. D **98**, 113002 (2018).
[44] N. G. Deshpande and E. Ma, Phys. Rev. D **18**, 2574 (1978).
[45] R. Barbieri, L. J. Hall, and V. S. Rychkov, Phys. Rev. D **74**, 015007 (2006).
[46] L. Lopez Honorez, E. Nezri, J. F. Oliver, and M. H. G. Tytgat, J. Cosmol. Astropart. Phys. 02 (2007) 028.
[47] L. Lopez Honorez and C. E. Yaguna, J. High Energy Phys. 09 (2010) 046.
[48] M. A. Díaz, B. Koch, and S. Urrutia-Quiroga, Adv. High Energy Phys. **2016**, 8278375 (2016).
[49] A. Vicente and C. E. Yaguna, J. High Energy Phys. 02 (2015) 144.
[50] V. Keus, S. F. King, S. Moretti, and D. Sokolowska, J. High Energy Phys. 11 (2014) 016.
[51] P. F. de Salas, D. V. Forero, S. Gariazzo, P. Martínez-Miravé, O. Mena, C. A. Ternes, M. Tórtola, and J. W. F. Valle, J. High Energy Phys. 02 (2021) 071.
[52] J. A. Casas and A. Ibarra, Nucl. Phys. **B618**, 171 (2001).
[53] T. Toma and A. Vicente, J. High Energy Phys. 01 (2014) 160.
[54] I. Cordero-Carrión, M. Hirsch, and A. Vicente, Phys. Rev. D **99**, 075019 (2019).
[55] I. Cordero-Carrión, M. Hirsch, and A. Vicente, Phys. Rev. D **101**, 075032 (2020).
[56] A. M. Baldini *et al.* (MEG Collaboration), Eur. Phys. J. C **76**, 434 (2016).
[57] M. Misiak, A. Rehman, and M. Steinhauser, J. High Energy Phys. 06 (2020) 175.
[58] Y. Amhis *et al.* (HFLAV Collaboration), arXiv:2206.07501.
[59] J. Grygier *et al.* (Belle Collaboration), Phys. Rev. D **96**, 091101 (2017); **97**, 099902(A) (2018).
[60] M. Tanabashi *et al.* (Particle Data Group), Phys. Rev. D **98**, 030001 (2018).